JOURNAL OF GEOPHYSICAL RESEARCH, VOL. 96, NO. C4, PAGES 7105–7113, APRIL 15, 1991

Slow-Time Modulation of Finite-Depth Nonlinear Water Waves: Relation to Longshore Current Oscillations

L. SHEMER,[1] N. DODD, AND E. B. THORNTON

Department of Oceanography, Naval Postgraduate School, Monterey, California

Nonlinear dynamics of steep waves in water of finite depth are analyzed. The most unstable Benjamin-Feir sidebands are found for a number of values of carrier wave steepness and water depth. The long-time evolution of a three-wave system, consisting of the carrier and the two most unstable sidebands, is then studied. Such a wave system undergoes periodic recurrence. It is shown that the slow-time modulation leads to a corresponding periodic variation in the radiation stress when the propagation directions of the sidebands differ from that of the carrier. The variation of the radiation stress, in turn, results in slow-time modulation of longshore current.

1. INTRODUCTION

In recent studies of low frequency waves in a surf zone of a barred beach during the 1986 SUPERDUCK experiment at Duck, North Carolina [*Crowson et al.*, 1988], considerable energetic motions were revealed in the horizontal velocity field along the shore. These waves were typically of $O(10^2$ m) and had periods which could exceed 10^3 s. Since these slow waves were shorter by an order of magnitude than the shortest possible surface gravity waves, known as infragravity edge waves, *Oltman-Shay et al.* [1989] suggested calling this band of nearshore wave energy the far-infragravity frequency band.

The first attempt to present a model of the far-infragravity waves was made by *Bowen and Holman* [1989]. They assumed that these waves result from the shear instability of the longshore current. The form and stability of the far-infragravity waves were strongly dependent on the beach topography and longshore current velocity profile. In order to attack the complicated natural phenomenon of temporal and spatial variability of longshore current, the shear instability approach considers a simplified model where the longshore current is essentially decoupled from the oncoming wavefield. The time-mean longshore current distribution as a function of the distance from the shore is assumed to be given a priori and serves as a starting point for the study of instability. The shear instability mechanism is thus independent of external forcing, and the possible time variation of the longshore current due to slow-time modulation of the wavefield is beyond the scope of shear instability studies. *Dodd and Thornton* [1990] and N. Dodd et al. (Shear instabilities in the longshore current: A comparison of observation and theory, submitted to *Journal of Physical Oceanography*, 1991) have further developed this approach and found reasonable agreement between the wave numbers and frequencies of the most unstable shear flow modes, and the experimental observations.

The omnipresence of the shear instabilities during SUPERDUCK stimulated interest in examining the results of the Nearshore Sediment Transport Study (NSTS) at Santa Barbara, California [see *Seymour*, 1989]. Although similar low-frequency, high-wave-number energy was observed at Santa Barbara, the organized motion exhibited by the dispersion curves of the shear instability was not noticed. This motivated investigations of alternative generation mechanisms. The temporal variations of the oncoming wave field can force corresponding variations in the longshore current by a number of possible mechanisms. It is well known that grouping of the oncoming swell may contribute significantly to low-frequency energy components in the surf zone [*Tucker*, 1950]. *Symonds et al.* [1982] related surf beat to the time-varying breakpoint due to the wave groups. *Tang and Dalrymple* [1989] have shown possible correlation between wave groups and rip currents.

The earlier studies of the forcing of the longshore current by the waves use an essentially linear approach. In contrast, in this paper we assume that the temporal variability of the longshore current may be forced by the nonlinear dynamics of steep water waves. In the absence of full understanding of the physics of the problem under considerations, it seems desirable to apply a simplest possible nonlinear model in order to check whether it is capable of describing the dominant features of the phenomenon. An attempt is thus made here to show the possible relation between the modulational instability of a finite-depth Stokes wave train and the slow-time variations in the radiation stress. We take advantage of the recent progress in nonlinear wave theory.

Mase and Iwagaki [1986] studied the wave grouping both experimentally and theoretically, using the nonlinear *Zakharov* [1968] wave evolution equation. They concluded that the wave grouping observed in a natural environment can be successfully described by applying the Zakharov model equation to the analysis of the Benjamin-Feir instability of the Stokes waves.

The Zakharov nonlinear wave equation employed by Mase and Iwagaki is the most general model equation describing slow-time evolution of deepwater gravity waves. The important advantage of the Zakharov equation is that it is not limited to a narrow wave spectrum, and thus one can consider the interactions between waves with quite different wave numbers and frequencies. This equation accounts for nonlinear interactions at the lowest possible order in the small parameter ε, which represents the wave steepness. For gravity waves, these interactions require coexistence of four

[1]Permanently at Department of Fluid Mechanics, Faculty of Engineering, Tel-Aviv University, Ramat-Aviv, Israel.

Paper number 91JC00061.
0148-0227/91/91JC-00061$05.00

resonating, or nearly resonating waves (the so-called quartet, or class I interactions), and they are of $O(\varepsilon^3)$. *Stiassnie and Shemer* [1984], hereinafter referred to as SS1, have rederived this equation for an arbitrary finite water depth. They have also extended the range of validity of the equation by including the so-called class II, i.e., five-wave resonant, or nearly resonant, interactions.

It is important to stress that in the derivation of the model equation by SS1 it is assumed that no near-resonant interactions of three waves (the so-called triad interactions) are possible. As is shown in a number of recent publications [e.g., *Elgar et al.*, 1990], these triad interactions may become dominant in shallow water ($kh \ll 1$). In the SS1 model the presence of triad interactions will manifest itself by notable singularities in the interaction coefficients. In order to eliminate these singularities, the present study is restricted to the region of validity of the model equation, i.e., water of intermediate depth.

The modified Zakharov equation was used by *Shemer and Stiassnie* [1985], hereinafter referred to as SS2, to study the long-time evolution of Stokes waves. Following the approach originally used by *Stiassnie and Kroszynski* [1982] for long-time evolution analysis based on the nonlinear Schrödinger equation, SS2 considered a three-wave system in deep water: a carrier and the two most unstable disturbances for both class I and class II interactions. It was found in these studies that such a wave system undergoes periodic modulation, where the initially weak sidebands grow at the early stages of the recurrence process, at the expense of the carrier, and then subdue again, completing the full recurrence period. This result is in agreement with the wave flume experiments of *Lake et al.* [1977] and large wave basin observations by *Su et al.* [1982]. Evolution of a wave packet power spectrum was studied by *Su* [1982] in a long tow tank. It was shown that the increase in the amplitude of the sidebands is accompanied indeed by simultaneous decrease in the power density of the carrier. As calculated by SS2, dimensionless recurrence periods $\omega_0 T_r$, where ω_0 is the radian frequency of the carrier, were $O(\varepsilon^{-2})$ for the class I interactions and $O(\varepsilon^{-3})$ for the class II interactions. For deepwater waves the recurrence periods for class II interaction are always notably longer than those for four-waves (class I) interactions. For extremely steep deep water waves the class I recurrence period can become shorter than 100 carrier wave periods.

Stiassnie and Kroszynski [1982] and *Stiassnie and Shemer* [1987] have studied the question of whether the truncated three-wave system can represent reliably the actual complicated wavefield. While these studies show that perfect periodicity is lost by considering additional wave components, the general behavior and the characteristic recurrence times in more complicated wave systems are still dominated by the most unstable modes.

The results of SS2 and *Mase and Iwagaki* [1986] for deepwater waves suggest that the Zakharov equation–based analysis of wave grouping due to Benjamin-Feir modulational instability in water of finite depth can shed some additional light on the experimentally observed temporal and spatial variations of the longshore current. It is important to note here that because of shoaling, the steepness of waves on the verge of breaking is very high, and the waves in this region can thus become strongly nonlinear. Under these circumstances, one can expect recurrence periods which are

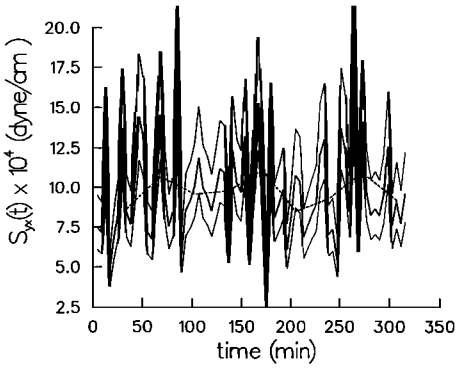

Fig. 1. Experimentally observed time modulation of 4.3-min averages of radiation stress (heavy line), with confidence intervals (light lines). The 34.1-min average of the radiation stress is shown as a dotted line.

of the order of magnitude of the typical longshore current variation periods. The assumption of constant water depth, which is intrinsic to the nonlinear theoretical model, can be justified in case of a beach with a mild slope.

2. Some Experimental Results

Motivation for this work is provided by an example of strongly modulated (in time) alongshore component of the radiation stress, S_{yx}, as shown in Figure 1. The solid heavy line is the radiation stress block averaged every 4.3 min. The 95% confidence limits (light lines) have been included to show that the variability is statistically significant. The mean modulation period is about 20 min, which represents an $O(10^2)$ waves of the narrow-band, 14-s carrier period. The 34.1-min block averages (dotted line) of the radiation stress are also indicated; although the total length of record is relatively short, an apparent longer modulation period of 100 min is suggested, which represents about 400 periods of the carrier in the modulation period.

The radiation stress was measured using a four-pressure-sensor, 610 square array (slope array) located in 9 m depth. The results are from measurements acquired during NSTS at Leadbetter Beach, Santa Barbara, California, in February 1980. The radiation stress was calculated by first calculating the cospectrum of the orthogonal slopes (η_x, η_y) of the sea surface, which is then converted to a velocity cospectrum and integrated over depth using a linear theory transfer function $H(f)$ [see *Higgins et al.*, 1981]

$$S_{yx}(f) = H(f)C_{\eta_x, \eta_y}(f) \tag{1}$$

The total radiation stress, the plot of which is shown in Figure 1, was calculated by integrating over the energetic region of the spectrum

$$S_{yx} = \int_{0\,05}^{0\,3} S_{yx}(f)\, df \tag{2}$$

Leadbetter Beach has an east-west orientation on a predominantly north-south coastline. The predominant wave direction is from the northwest. The incident waves from the open ocean must pass through a narrow passage between Point Conception and San Miguel Island, limiting the range of admissible angles to be 240°–258° and resulting in a narrow band (in both direction and frequency) of energy arriving

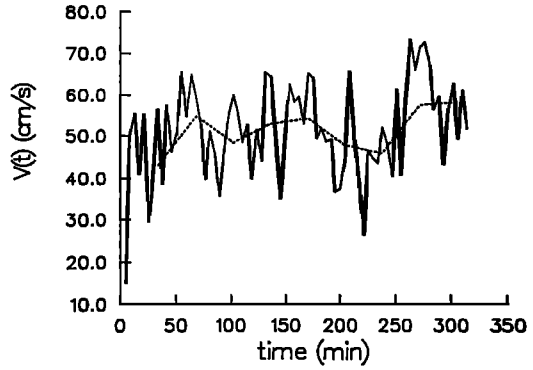

Fig. 2. Experimentally observed time modulation of longshore current (4.3-min averages, solid line; 34.1-min averages, dotted line).

from the open ocean at relatively large angles to the beach [see *Guza et al.*, 1986]. This was the case for February 4, for which the energy density, radiation stress, and mean angle spectra were calculated using 34.1-min records. The waves were narrow banded with a 14-s peak period and corresponding mean wave direction of 20° to the beach normal. The nondimensional depth is $k_0h = 0.4$, where k_0 corresponds to the wave length at the peak of the spectrum calculated using linear theory. The rms amplitude of the waves was 0.26 m, giving a wave slope $a_{\text{rms}}k_0 = 0.01$. Assuming a Rayleigh distribution for wave amplitudes gives $a_{\max} \simeq 2a_{\text{rms}}$, resulting in a maximum wave slope of 0.02.

The longshore current was relatively strong ($V_{\max} = 1$ m/s) as a result of the relatively large incidence angles of the waves to the beach. The modulated radiation stress resulted in a modulated longshore current (Figure 2). *Guza et al.* [1986] examined the waves and currents on this beach over an 18-day period and found that the longshore current was highly correlated with the total radiation stress (correlation coefficient = 0.97). The reason for the high correlation is that the primary driving force for the longshore current is the cross-shore gradient of S_{yx}. The radiation stress is conserved up to wave breaking and goes to zero at the shoreline. Therefore the total S_{yx} before breaking divided by the surf zone width is a measure of the gradient across the entire surf zone and would be expected to be related to the longshore current.

3. Theoretical Background

3.1. *Outline of the Theoretical Approach*

We consider an initially nearly monochromatic nonlinear Stokes wave train (the carrier), which propagates in water of finite depth. Water depth ranging from nearly shallow to intermediate depth is considered. The steepest theoretically possible wave height $H_{\max}$ for any constant water depth was given by *Cokelet* [1977]. Since we are dealing with waves close to breaking, steep wave trains are considered, with the carrier wave heights in the range $0.5H_{\max} < H_0 < H_{\max}$. The wave height H_0 is then translated to the amplitude of the first term in the Stokes expansion, a_0, using the expression truncated to the third order, of *Skjelbreia and Hendrickson* [1961]:

$$\frac{k_0H_0}{2} = k_0a_0\left[1 + \frac{24\cosh^6(k_0h) + 3}{64\sinh^6(k_0h)}(k_0a_0)^2\right] \tag{3}$$

where $k_0 = |\mathbf{k}_0|$ is the magnitude of the carrier wave number.

For each water depth and carrier wave steepness considered, the most linearly unstable sidebands are then determined using the Zakharov equation. It is then assumed that the wavefield is dominated by three waves, the carrier and the two most unstable sidebands. The long-time evolution of such a wave system is thus computed, again using the Zakhavor equation. The dependence of modulation period and depth on the input parameters is established. At the last stage, the linear approximation is adopted for each wave separately, and the modulation of the radiation stress is calculated, following the procedure adopted in the experiments.

3.2. *Zakharov Equation*

The Zakharov equation describes the temporal evolution of a gravity wave propagating in an incompressible inviscid fluid with a free surface at $z = \eta(\mathbf{x}, t)$ and bottom at $z = -h$. The velocity potential $\phi(\mathbf{x}, z, t)$ satisfied the Laplace equation, $\eta(\mathbf{x}, t)$ and $\phi(\mathbf{x}, z, t)$ satisfy the kinematic and dynamic boundary conditions at the free surface, and $\partial\phi/\partial z = 0$ at $z = -h$. The evolution equation in Fourier space, valid to $O(\varepsilon^3)$, has the following form:

$$i\frac{\partial B_0}{\partial t} = \int\int\int_{-\infty}^{\infty} T_{0123}B_1^*B_2B_3\,\delta(\mathbf{k}_0 + \mathbf{k}_1 - \mathbf{k}_2 - \mathbf{k}_3) \cdot \exp[i(\omega_0 + \omega_1 - \omega_2 - \omega_3)t]\,d\mathbf{k}_1\,d\mathbf{k}_2\,d\mathbf{k}_3 \tag{4}$$

where the nonlinear interaction coefficient $T_{0123} = T(\mathbf{k}_0, \mathbf{k}_1, \mathbf{k}_2, \mathbf{k}_3, h)$ is given by a quite lengthy expression in SS1 and the frequencies are related to the absolute value of the wave number $k_j = |\mathbf{k}_j|$ by the linear dispersion relation $\omega_j^2 = gk_j\tanh(k_jh)$. The amplitudes $B_j = B(\mathbf{k}_j, t)$ are the linear parts of the complex spectral "amplitudes" b_j, which are related to the Fourier components in the wave number space (denoted by a circumflex) of the surface elevation $\eta(\mathbf{x}, t)$ and the velocity potential at the free surface $\phi^S[\mathbf{x}, \eta(\mathbf{x}, t), t]$:

$$b(\mathbf{k}, t) = \left[\frac{g}{2\omega(k)}\right]^{1/2}\hat{\eta}(\mathbf{k}, t) + i\left[\frac{\omega(k)}{2g}\right]^{1/2}\hat{\phi}^S(\mathbf{k}, t) \tag{5}$$

3.3. *Linear Stability Analysis*

Equation (4) is now used to study the linear stability of the wave train B_0. Following *Crawford et al.* [1981] and SS1, we assume that the carrier and the disturbances B_1 and B_2 have the following wave numbers:

$$\mathbf{k}_0 = k_0(1, 0) \qquad \mathbf{k}_1 = k_0(1 + p, q)$$
$$\mathbf{k}_2 = k_0(1 - p, -q) \tag{6}$$

Note that in all computational results presented subsequently it is assumed without loss of generality that $k_0 = 1$. The system of four waves with the wave numbers given by (6), which includes the carrier B_0 taken twice, and both sidebands, satisfies the δ-function condition on the wave

numbers in (4), i.e., $2\mathbf{k}_0 = \mathbf{k}_1 + \mathbf{k}_2$. Equations (4) linearized with respect to the sidebands for B_1 and B_2 are:

$$i\frac{dB_1}{dt} = 2T_{1010}|B_0|^2B_1 + T_{1200}B_0^2B_2^* \exp[-i(2\omega_0 - \omega_1 - \omega_2)t] \quad (7a)$$

$$i\frac{dB_2}{dt} = 2T_{2020}|B_0|^2B_2 + T_{2100}B_1^*B_0^2 \exp[-i(2\omega_0 - \omega_1 - \omega_2)t] \quad (7b)$$

The solution of equations (7), which are linear with respect to B_1 and B_2, has the following form:

$$B_1 = b_1 \exp\{-i[0.5(2\omega_0 - \omega_1 - \omega_2) + \Omega]t\} \quad (8a)$$

$$B_2 = b_2 \exp\{-i[0.5(2\omega_0 - \omega_1 - \omega_2) - \Omega]t\} \quad (8b)$$

where

$$\Omega = (T_{1010} - T_{2020})|B_0|^2 \pm D^{1/2} \quad (9a)$$

and the discriminant of the second-order algebraic equation is given by

$$D = \left(\frac{2\omega_0 - \omega_1 - \omega_2}{2} - (T_{1010} + T_{2020})|B_0|^2\right)^2 - T_{1200}T_{2100}|B_0|^4 \quad (9b)$$

The solutions (8) are unstable when $\mathrm{Im}(\Omega) \neq 0$ (i.e., $D < 0$); $D(p, q) = 0$ defines the stability boundaries in the (p, q) plane, and the most unstable mode is defined by the maximum of $-D$: $D(p_{\max}, q_{\max}) = D_{\min}$.

3.4. *Long-Time Evolution*

Following SS2, we now consider the long-time evolution of a three-wave system consisting of waves with the wave numbers given by (6) and with the initial amplitudes and phases

$$a_0(0) = \hat{a}_0 \quad a_j(0) = \mu_j\hat{a}_0 \quad \mu_j \ll 1 \quad j = 1, 2 \quad (10a)$$

$$\theta(0) = 0 \quad \theta_j(0) = \hat{\theta}_j \quad (10b)$$

where the amplitudes a_j and phases θ_j are related to the complex "amplitudes" B_j by

$$B_j(0) = \pi(2g/\omega_j)^{1/2} a_j(0) \exp[i\theta_j(0)] \quad (11)$$

The selection of the three-wave system consisting of the carrier and the most unstable sidebands is based on the conclusion of *Stiassnie and Kroszynski* [1982] that this truncated system, while being simple enough for analysis, still provides a reliable pattern of the general behavior of much more complicated wave systems. The nonlinear evolution of B_j is described by a system of discretized equations (4):

$$i\frac{dB_0}{dt} = (T_{0000}|B_0|^2 + 2T_{0101}|B_1|^2 + 2T_{0202}|B_2|^2)B_0 + 2T_{0012}B_0^*B_1B_2 \exp[i(2\omega_0 - \omega_1 - \omega_2)t] \quad (12a)$$

$$i\frac{dB_1}{dt} = (T_{1111}|B_1|^2 + 2T_{1010}|B_0|^2 + 2T_{1212}|B_2|^2)B_1 + T_{1200}B_2^*B_0^2 \exp[-i(2\omega_0 - \omega_1 - \omega_2)t] \quad (12b)$$

$$i\frac{dB_2}{dt} = (T_{2222}|B_2|^2 + 2T_{2020}|B_0|^2 + 2T_{2121}|B_1|^2)B_2 + T_{2100}B_1^*B_0^2 \exp[-i(2\omega_0 - \omega_1 - \omega_2)t] \quad (12c)$$

The system of ordinary differential equations (12) can be solved either analytically, using the Jacobian elliptic functions [see SS2], or by direct numerical integration, following *Stiassnie and Shemer* [1987]. These two independent methods of solution can be used to verify the accuracy of the procedure. As was shown by SS2, analytically, the evolution of the wave system is periodic in time. The recurrence period is determined from the solution of (12).

3.5. *Radiation Stress*

The radiation stress, to the lowest order, is related to the jth wave energy E_j and the wave incidence angle α_j by

$$(S_{yx})_j = E_j\frac{k_j}{\omega_j}(c_g)_j \sin\alpha_j \cos\alpha_j \quad (13)$$

where c_g is the wave group velocity [*Longuet-Higgins*, 1970]. Once the long-time evolution of the nonlinear wave system given by (6) and (10) is determined, the problem is studied at each instant during the modulation period at the linear level, i.e., using (13) to determine the radiation stress for each wave separately, thus yielding the total radiation stress at a given instant,

$$S_{yx}(t) = \sum_{j=1}^{3}[S_{yx}(t)]_j \quad (14)$$

The energy E_j is given at the lowest order by [*Stiassnie and Shemer*, 1987]

$$E_j = \frac{1}{4\pi^2}\omega_j|B_j|^2 \quad (15)$$

Stiassnie and Shemer [1987] have also shown that in order to improve substantially the accuracy of the energy calculations, higher-order terms have to be included in the evolution equations (12). The contribution to the total energy of the bounded waves resulting from the nonlinear interactions between the waves has also to be accounted for. Such an endeavor is beyond the scope of the present paper. The indications regarding the accuracy of (15) can be obtained, however, by considering the total energy of the three-wave system, as computed using (15). Since the Zakharov equation describes the energy-conserving Hamiltonian system, variations of the total equation during the modulation process can serve as a measure of accuracy of the adopted approximation.

Owing to conservation of the total energy in the modulation process, the cases where the propagation direction of the most unstable sidebands differs from that of the carrier are of main interest in the present context.

TABLE 1. Parameters of the Most Unstable Modes and the Corresponding Recurrence Periods

k_0h	a_0k_0	p_{max}	q_{max}	$\omega_0T/2\pi$
0.36	0.066	0.429	0.313	15.6
	0.0528	0.488	0.271	36.1
	0.033	0.546	0.211	114.7
	0.02	0.543	0.177	587.3
0.51	0.123	0.492	0.326	27.6
	0.0984	0.523	0.291	49.0
	0.0615	1.145	0.0	98.0
0.69	0.19	1.258	0.0	23.1
	0.152	1.227	0.0	38.0
	0.095	1.194	0.0	104.9
0.92	0.26	1.250	0.0	38.2
	0.208	1.247	0.0	60.5
	0.13	1.244	0.0	157.3
1.2	0.322	0.396	0.219	66.0
	0.2576	0.370	0.222	77.5
	0.161	0.310	0.209	145.3
1.4	0.351	0.392	0.199	48.1
	0.2808	0.372	0.212	58.6
	0.1755	0.306	0.205	113.8
∞	0.416	0.601	0.0	29.0
	0.3328	0.464	0.0	32.4
	0.208	0.316	0.0	61.9

4. COMPUTATIONAL RESULTS

The summary of the linear stability results based on solution of (9) is given in Table 1, while the domains of instability in p-q space for some representative cases are presented in Figure 3. The calculations were performed for the dimensionless mean depth values k_0h which correspond to those used by *Cokelet* [1977]. The results in Table 1 are presented at each mean water depth for three carrier wave steepness values, which are close to 100%, 80%, and 50% of the maximum possible wave steepness at the given depth, as given by Cokelet. The single exception is the inclusion of the results for $k_0h = 0.36$ and $a_0k_0 = 0.02$, which are in close agreement with the actual parameters in the field experiments reported in section 2.

For the deep water, there is a single domain of instability, and the most unstable modes have $q = 0$ and thus the propagation direction identical with that of the carrier, the so-called two-dimensional instability (Figure 3*a*). This result of the model is in good agreement with the exact solution of *McLean* [1982*a*]. For water of intermediate depth, $k_0h = 1.4$, there are important changes in the stability diagram given in Figure 3*b*: the most unstable mode now has $q \neq 0$, thus corresponding to three-dimensional disturbances, and the domain of instability now appears to consist of two separate domains. Following SS1, we will refer to the larger domain adjacent to the q axis as the main domain, and to the smaller instability region at higher values of p as the secondary domain. As was discussed by SS1, the existence of the secondary instability domains may stem from the model approximations, since these domains are not shown explicitly in *McLean*'s [1982*b*] exact solution.

Figures 3*c* and 3*d* show the effects of the carrier amplitude on the stability diagram at $k_0h = 0.69$. In contrast to Figure 3*b*, the most unstable mode now is in the secondary region and has the transverse wave number component $q = 0$, thus being two-dimensional. This result is again in agreement with *McLean* [1982*b*]. For even more shallow water, $k_0h = 0.36$, the shape of the instability domain (Figures 3*e* and 3*f*) remains similar to the previous case, but the most unstable modes are three-dimensional again. There is thus a range of k_0h where the most unstable disturbances are in the secondary instability region and have $q = 0$, while beyond this range, finite-depth Stokes waves are most unstable to three-dimensional disturbances. At $k_0h = 0.51$, the most unstable disturbance for steep waves is three-dimensional, while for relatively mild wave steepness of 0.0615, the transverse wave number component $q = 0$. The transition boundaries between the two- and three-dimensional 3D instabilities in the wave steepness–mean depth space were delineated in SS1.

Table 1 also presents the long-time modulation periods (in terms of the carrier wave periods) of the three-wave system defined by (6), for various water depths and steepnesses. The initial amplitude of the sidebands was in these computations chosen to be $\mu_1 = \mu_2 = 0.1$, and the initial phase angles of the disturbances were $\theta_1 = \theta_2 = 0$. The modulation periods for the steepest possible wave are in the range of 15 to 66 carrier wave periods and are correspondingly longer for less steep waves. The calculated modulation period for $k_0h = 0.36$ and $a_0k_0 = 0.02$ is of the same order of magnitude as the experimentally measured value (compare Figure 1).

As was mentioned above, we are mainly interested in the long-time evolution of a finite-depth wavetrain most unstable to three-dimensional disturbances. The study of the effects of the initial conditions on the modulation process is presented thus in Figure 4 for $k_0h = 1.2$ and $a_0k_0 = 0.258$, which correspond to 80% of the maximum possible wave steepness (see Table 1). Figure 4*a* shows the slow-time variation of the amplitudes of the three waves considered when the initial amplitudes of the sideband disturbances are both identical and equal to 0.1 of the carrier and all initial phase angles are assumed to be zero. The modulation pattern, however, remains qualitatively the same for other initial conditions. Figure 4*b* demonstrates that it is sufficient to have only one sideband present at the initial stage, and its counterpart is generated in the nonlinear interaction process during the long-time evolution. The modulation period in this case is by about 20% longer than that in Figure 4*a*, where both sidebands were present initially. Figure 4*c* shows that the initial phase of the disturbances can also affect the modulation process. In this case the initial amplitude of the sidebands is identical to that of Figure 4*a*, but the phase angles are now $\hat{\theta}_1 = \hat{\theta}_2 = \pi/4$. The sidebands in Figure 4*c* initially decay, and the carrier amplitude grows at the expense of the sidebands and attains maximum above the initial value, but then the modulation resumes its familiar shape. The recurrence period is here again longer than that in Figure 4*a*. Finally, when both sidebands are weak initially, $\mu_1 = \mu_2 = 0.01$ in Figure 4*d*, the modulation period becomes nearly twice as long as with stronger initial disturbance. All these examples therefore demonstrate that recurrence periods are only weakly dependent on the initial conditions, retaining the same order of magnitude for a wide range of amplitudes and phases of the most unstable disturbance. In all cases considered, the maximum amplitudes attained by the sidebands are quite similar. This is in agreement with the deep water wave study by *Stiassnie and Shemer* [1987].

As was already noticed, the long-time modulation of the

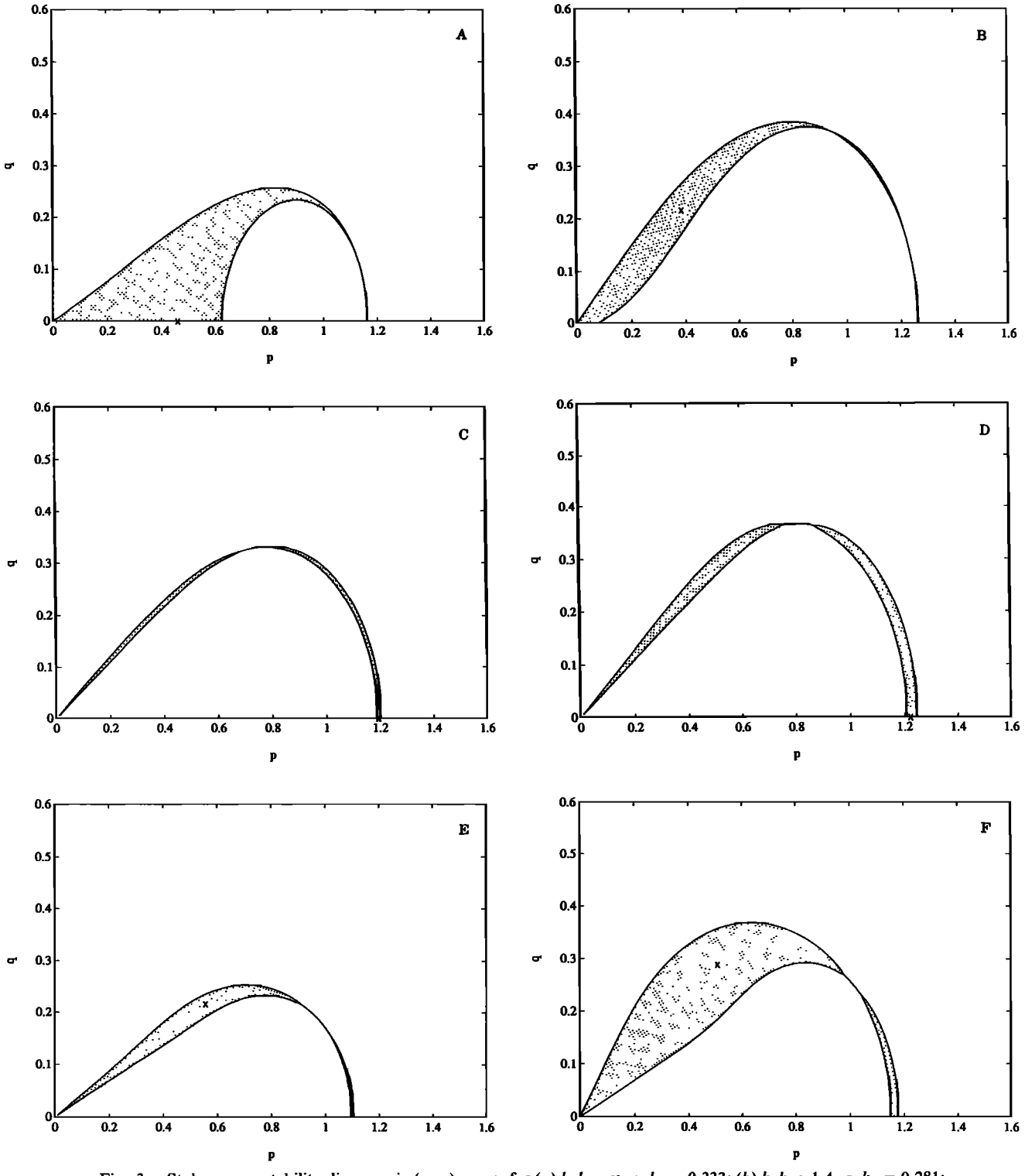

Fig. 3. Stokes wave stability diagrams in (p, q) space, for (*a*) $k_0h = \infty$, $a_0k_0 = 0.333$; (*b*) $k_0h = 1.4$, $a_0k_0 = 0.281$; (*c*) $k_0h = 0.69$, $a_0k_0 = 0.095$; (*d*) $k_0h = 0.69$, $a_0k_0 = 0.152$; (*e*) $k_0h = 0.36$, $a_0k_0 = 0.033$; and (*f*) $k_0h = 0.36$, $a_0k_0 = 0.053$. Shaded regions indicate regions of instability. Crosses show the position of the fastest growing unstable mode.

wavefield can result in corresponding variation of the total radiation stress only when the sidebands have a nonzero wave number component in the direction perpendicular to the carrier wave propagation. The temporal variation of the total radiation stress S_{yx} computed at each instant according to (13) to (15), is presented in Figure 5*a* for intermediate depth, $k_0h = 1.2$, and in Figure 5*b* for shallower water, $k_0h = 0.51$. The time dependence of S_{yx} for both water depths is given for two values of the incidence angle, 5° and 30°. One can see that long-time modulation of the finite-depth Stokes wave train, which results from the Benjamin-Feir instability, can indeed lead to considerable temporal variations in the radiation stress. Note that in both cases presented in Figure 5, the modulation of S_{yx} was much

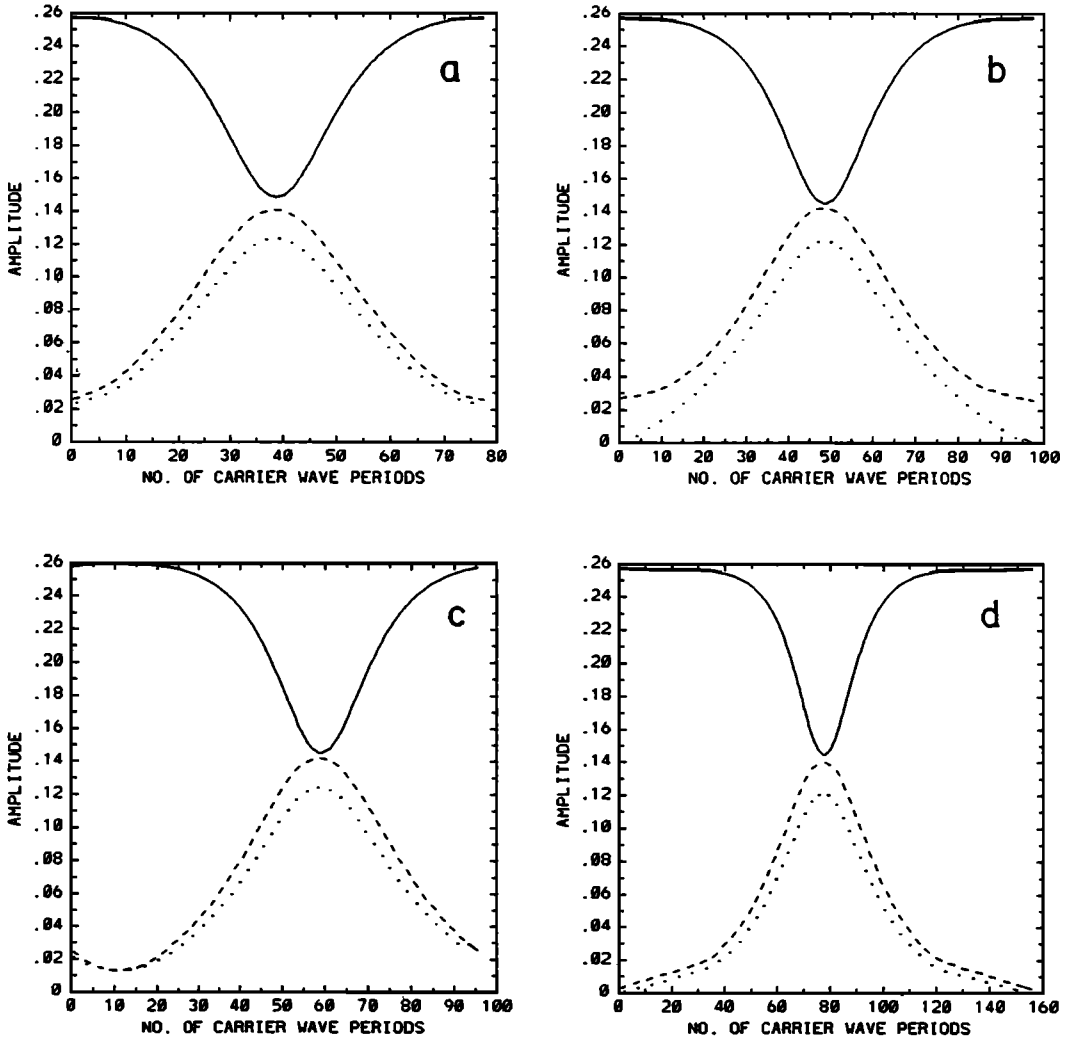

Fig. 4. Amplitudes of carrier and sidebands over one modulation period for $k_0h = 1.2$ and $a_0k_0 = 0.258$: (*a*) $\mu_1 = 0.1$, $\mu_2 = 0.1$, $\theta_1 = 0$, $\theta_2 = 0$; (*b*) $\mu_1 = 0.1$, $\mu_2 = 0.0$, $\theta_1 = 0$, $\theta_2 = 0$; (*c*) $\mu_1 = 0.1$, $\mu_2 = 0.1$, $\theta_1 = \pi/4$, $\theta_2 = \pi/4$; and (*d*) $\mu_1 = 0.01$, $\mu_2 = 0.01$, $\theta_1 = 0$, $\theta_2 = 0$.

deeper than the apparent variation in the total wave energy as calculated using the linear approximation (15). This approximation is quite satisfactory for $k_0h = 1.2$, giving the total change in the wave energy in course of the modulation process not exceeding a few percent. The lowest-order energy calculation in shallow water ($k_0h = 0.51$) is of course less accurate, but even in this case the relative range of variations in S_{yx} is larger by about a factor of 2 than that of the total energy.

5. Discussion and Summary

The present study does not attempt to perform a quantitative comparison between the experimental results and the theoretical analysis. On the one hand, the wave's stationarity is insufficient for the long periods of time in the field measurements, while on the other hand, application of the Zakharov nonlinear equation necessarily demands adoption of some restrictive assumptions, as was discussed above. Nevertheless, there exists a reasonable similarity between the computational results presented here and the experiments.

The theoretical analysis clearly indicates that in water of finite depth the Benjamin-Feir instability of a steep Stokes wave train can lead to a strong, periodic, three-dimensional long-time modulation of the wavefield and resulting variation in S_{yx}. The period of such a modulation is of the order of 10–10^2 carrier wave periods, and is thus close to the modulation periods in S_{yx} as given in Figure 1. The amount of modulation (see Figure 5), while being dependent on the chosen set of parameters, also resembles the field measurements. Moreover, the transverse wave number components for all parameters where the modulational instability is three-dimensional are in the range $0.2 < q < 0.35$. Hence the length scale of variations in the direction normal to the carrier wave propagation is between 3 and 5 carrier wave lengths. This again, is in agreement with the experiments of *Oltman-Shay et al.* [1989].

For water depth values where the most unstable disturbances are three-dimensional, the present work thus suggests a mechanism for the observed slow variations in the radiation stress and the resulting longshore current. It is, however, plausible to assume that in the range of the depth

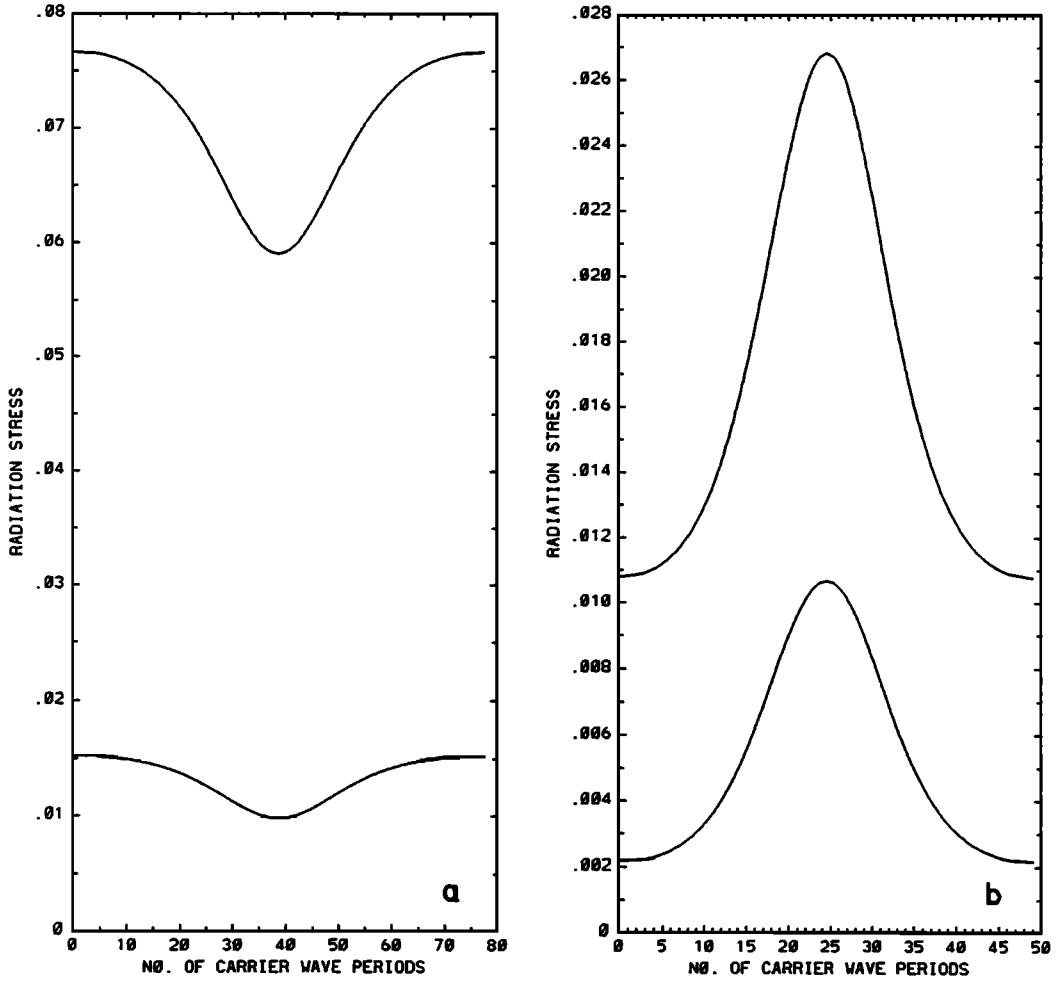

Fig. 5. Variation of S_{yx} over one modulation period: (*a*) $k_0h = 1.2$, $a_0k_0 = 0.258$, $\mu_1 = \mu_2 = 0.1$, $\theta_1 = \theta_2 = 0$; (*b*) $k_0h = 0.51$, $a_0k_0 = 0.098$, $\mu_1 = \mu_2 = 0.1$, $\theta_1 = \theta_2 = 0$.

about $0.5 < k_0h < 0.95$, where the Benjamin-Feir instability is two-dimensional and thus does not lead to temporal variations in the radiations stress, the wave grouping due to long-time modulation of the dominant wave system breaking at oblique incident angles to the beach can also result in variations in time of the longshore current. The present results indicate that the actual changes of the wave amplitudes in the course of the modulation process, which have periods similar to those in the three-dimensional case (see Table 1) can on a sloped beach lead to corresponding temporal variations in the location of the breaking line, as was discussed by *Symonds et al.* [1982], and thus in the longshore current.

In summary, the present work suggests that the nonlinear resonant interactions of steep waves in water of finite depth in the nearshore region under certain conditions can constitute one of the possible physical mechanisms for slow temporal variations in the longshore current, as observed in recent experiments. Additional detailed experimental field work is necessary to determine the actual importance of the suggested mechanism as compared to the alternatives. In particular, in seems interesting to study experimentally the temporal variation of the short-time directional spectra of the wavefields at different phases of the assumed recurrence process, under conditions when the modulation of the longshore current can actually be recorded. These spectra should be calculated over durations which are long compared to the dominant wave periods, but short relative to the expected in the present model modulation periods. Such experimental data can provide an indication of whether the nonlinear interactions that result in simultaneous temporal variations in the amplitudes of the carrier and the most unstable sidebands can be related indeed to the slow-time modulation of the longshore current, as is suggested in the present study.

Acknowledgments. This work was carried out while L.S. held a National Research Council–NPS Senior Research Associateship. N.D. and E.B.T. were supported by the Office of Naval Research and the Naval Postgraduate School.

REFERENCES

Bowen, A. J., and R. A. Holman, Shear instabilities of the mean longshore current, 1, Theory, *J. Geophys. Res.*, *94*, 18,023–18,030, 1989.

Cokelet, E. D., Steep gravity waves in water of arbitrary uniform depth, *Philos. Trans. R. Soc. London, Ser. A*, *286*, 183–230, 1977.

Crawford, D. R., B. M. Lake, P. G. Saffman, and H. C. Yuen, Stability of weakly nonlinear deep-water waves in two and three dimensions, *J. Fluid Mech.*, *105*, 177–191, 1981.

Crowson, R. A., W. A. Birkemeier, H. M. Klein, and H. C. Miller, SUPERDUCK nearshore processes experiment: Summary of

studies, *Tech. Rep. CERC-88-12*, Coastal Eng. Res. Cent. Field Res. Facil., Washington, D.C., 1988.

Dodd, N., and E. B. Thornton, Growth and energetics of shear waves in the nearshore, *J. Geophys. Res.*, *95*, 16,075–16,083, 1990.

Elgar, S., M. H. Freilich, and R. T. Guza, Recurrence in truncated Boussinesq models for nonlinear waves in shallow water, *J. Geophys. Res.*, *95*, 11,547–11,556, 1990.

Guza, R. T., E. B. Thornton, and N. Christensen, Jr., Observation of steady longshore currents in the surf zone, *J. Phys. Oceanogr. 16*, 1959–1969, 1986.

Higgins, A. L., R. J. Seymour, and S. S. Pawka, A compact representation of ocean wave directionality, *Appl. Ocean Res.*, *3*, 105–111, 1981.

Lake, B. M., H. C. Yuen, H. Rungaldier, and W. E. Ferguson, Nonlinear deep water waves: Theory and experiment, 2, Evolution of a continuous wave train, *J. Fluid Mech.*, *83*, 49–74, 1977.

Longuet-Higgins, M.S., Longshore currents generated by obliquely incident sea waves, *J. Geophys. Res.*, *75*, 6778–6789, 1970.

Mase, H., and Y. Iwagaki, Wave group analysis of natural wind waves based on modulational instability theory, *Coastal Eng.*, *10*, 341–354, 1986.

McLean, J. W., Instabilities of finite-amplitude water waves, *J. Fluid Mech.*, *114*, 315–330, 1982*a*.

McLean, J. W., Instabilities of finite-amplitude gravity waves on water of finite depth, *J. Fluid Mech.*, *114*, 331–341, 1982*b*.

Miller, I., and J. E. Freund, *Probability and Statistics for Engineers*, 530 pp., Prentice-Hall, Englewood Cliffs, N. J., 1985.

Oltman-Shay, J., P. A. Howd, and W. A. Birkemeier, Shear instabilities of the mean longshore current, 2, Field observations, *J. Geophys. Res.*, *94*, 18,031–18,042, 1989.

Seymour, R. J., (Ed.), *Nearshore Sediment Transport*, 418 pp., Plenum, New York, 1989.

Shemer, L., and M. Stiassnie, Initial instability and long-time evolution of Stokes waves, in *The Ocean Surface: Wave Breaking, Turbulent Mixing and Radio Probing*, edited by Y. Toba and H. Mitsuyasu, pp. 51–57, D. Reidel, Norwell, Mass., 1985.

Skjelbreia, L., and J. Hendrickson, Fifth order gravity wave theory, *Proc. Conf. Coastal Eng.*, *7th*, (1), 184–196, 1961.

Stiassnie, M., and U. I. Kroszynski, Long-time evolution of an unstable water-wave train, *J. Fluid Mech.*, *116*, 207–225, 1982.

Stiassnie, M., and L. Shemer, On modifications of the Zakharov equation for surface gravity waves, *J. Fluid Mech.*, *143*, 47–67, 1984.

Stiassnie, M., and L. Shemer, Energy computations for evolution of class I and II instabilities of Stokes waves, *J. Fluid Mech.*, *174*, 299–312, 1987.

Su, M.-Y., Evolution of groups of gravity waves with moderate to high steepness, *Phys. Fluids*, *25*, 2167–2174, 1982.

Su, M.-Y., M. Bergin, P. Marler, and R. Myrick, Experiments on non-linear instabilities and evolution of steep gravity-wave trains, *J. Fluid Mech.*, *124*, 45–72, 1982.

Symonds, G., D. A. Huntley, and A. J. Brown, Two-dimensional surf beat: Long wave generation by a time-varying breakpoint, *J. Geophys. Res.*, *87*, 492–498, 1982.

Tang, E. C.-S., and R. A. Dalrymple, Rip currents and wave groups, in *Nearshore Sediment Transport*, edited by R. J. Seymour, pp. 205–230, Plenum, New York, 1989.

Tucker, M. J., Surf beats: Sea waves of 1 to 5 minute period, *Proc. R. Soc. London, Ser. A*, *202*, 565–573, 1950.

Zakharov, V. E., Stability of periodic waves of finite amplitude on the surface of a deep fluid, *J. Appl. Mech. Tech. Phys.*, (Engl. transl.), *9*, 190–194, 1968.

N. Dodd and E. B. Thornton, Department of Oceanography, Naval Postgraduate School, Monterey, CA 93943.

L. Shemer, Department of Fluid Mechanics and Heat Transfer, Tel Aviv University, Ramat-Aviv 69978, Israel.

(Received October 9, 1990;
revised December 31, 1990;
accepted December 31, 1990.)